energies

MDPI

Article

Pool Boiling Heat Transfer Coefficient of Low-Pressure Glow Plasma Treated Water at Atmospheric and Reduced Pressure

Bartosz Gil *, Zbigniew Rogala and Paweł Dorosz

Faculty of Mechanical and Power Engineering, Wroclaw University of Science and Technology, wybrzeże Stanisława Wyspiańskiego 27, 50-370 Wrocław, Poland; zbigniew.rogala@pwr.edu.pl (Z.R.); pawel.dorosz@pwr.edu.pl (P.D.)

* Correspondence: bartosz.gil@pwr.edu.pl

Received: 25 November 2019; Accepted: 18 December 2019; Published: 21 December 2019

Abstract: This paper investigates the influence of low-pressure glow plasma water treatment on boiling phenomenon. The presented results show the novel influence and potential new applications of low-pressure glow plasma treated water. Low-pressure glow plasma water treatment affects some of its physical properties such as surface tension, pH, and electric conductivity; this is due to changes in the water structure. An experimental analysis aimed to investigate the effect of such a treatment on the boiling heat transfer coefficient of water, and to assess the stability of GPTW. The experiments were carried out at atmospheric and reduced pressure for heat fluxes up to 70 kW/m^2. The analysis shows significant deterioration of the boiling heat transfer coefficient under reduced pressure. In addition, the plasma treatment process had no significant effect on the thermal conductivity of water, as confirmed experimentally. A slight increase was observed, but it was within the measuring error range of the instruments used.

Keywords: heat transfer coefficient; natural refrigerant; water; pool boiling; low-pressure glow plasma; thermal conductivity

1. Introduction

The phenomenon of boiling plays a vital role in various branches of industry. The effects on the boiling process have various parameters, related to the properties of the boiling liquid, the characteristics of the heating surface, and the way these interact. Although the boiling phenomenon has not been fully researched and described, we are able to effectively use the thermal effects that accompany it to meet our needs. This does not mean, however, that it is not worth striving for a fuller understanding of the boiling process. A more detailed description will allow more precise predictions to be made of the thermal effects associated with this phenomenon. This will, in turn, make it possible to optimize the design process and operation of equipment and systems using boiling of working substances. It should be noted that among natural working fluids, substances with extremely different characteristics and applications in refrigeration technology can be found. Each of the natural refrigerants has some advantages and disadvantages: hydrocarbons have flammable properties, ammonia is a highly toxic, carbon dioxide has a relatively low heat of evaporation and high working pressures, and water has a very high boiling point at normal pressure. All of these working fluids also have unique advantages, due to their thermodynamic and physical properties, availability, or price.

The unquestionable advantages of water as refrigerant are its high heat of evaporation and lack of toxicity and destructive influence on the ozone layer. Due to its very high boiling point, water is not applicable to classic, compressor refrigeration systems. However, with the development of

sorption refrigeration, (in particular LiBr/H_2O devices), water as a refrigerant finds wider application in the refrigeration branch. Although water is one of the most commonly-encountered and the most thoroughly researched substances, also in terms of its use in refrigeration, scientists' efforts to discover its hitherto unknown properties or to modify those already researched do not cease. Water, as one of the most common substances on earth, is popular in industrial and power engineering applications such as combined heat and power (CHP), multi-effect desalination (MED) [1], adsorption [2,3], absorption [4,5], or ejector cooling systems [6]. All these applications struggle with the low heat transfer coefficient of water under reduced pressure. Water is not only an ecofriendly, safe, and cheap refrigerant, but it also possesses distinctive heat capacity properties. Moreover, it exhibits good boiling heat transfer performance, which is, however, significantly deteriorated at subatmospheric pressures [7].

As the performance of the aforementioned technologies strongly depend on boiling heat transfer performance, the issue of increasing boiling heat transfer coefficients becomes of the great importance. Plenty of techniques to enhance the boiling heat transfer coefficients of water have been proposed, mainly concerning heat transfer surface modification [8–11] or the addition of nanoparticles (so called nanofluids) [12,13]. Jones et al. [14] performed experimental studies of the effects of surface roughness on nucleate pool boiling heat transfer. It was concluded that rough surfaces can significantly improve the boiling heat transfer coefficient. Mori et al. [8] investigated the influence of nanoparticle-coating and honeycomb porous plates on the enhancement of critical heat flux. Honeycomb porous plates were found to significantly increase the critical heat flux, while the application of nanoporous-coating deteriorate it. The effect of the application of composite porous surface on the boiling heat transfer of deionized water is reported in [9]. Such a surface modification also enhances the boiling heat transfer coefficients. Yang et al. [15] examined copper foam covers and found them to effectively increase the boiling heat transfer coefficient, especially in the case of small cover thickness. Shi et al. [16] reported an increased boiling heat transfer coefficient using copper nanowire arrays. The heat transfer coefficients increased with an increase of nanowire length. Wang et al. [17] proposed a chemically-patterned surface which increased the heat transfer coefficient by about 22% in comparison to a homogenous hydrophilic microchannel. Finally, McGillis et al. [18] presented an analysis of the application fins on a water pool boiling at low pressure. The presented modifications enhanced the boiling heat transfer for wall superheat greater than 5 K. You et al. [19] investigated the effect of the addition nanoparticles on the critical heat flux of water. The critical heat flux was increased greatly, but there was no visible increase in the heat transfer coefficients within a wall superheat range of up to 20 K. Another study [20] showed that in cases of greater nanoparticle concentrations, the boiling heat transfer coefficient could be significantly reduced. Similar results were obtained for boiling water with 0.1 vol% titania in [21]. Finally, Chopkar et al. [22] reported improved boiling heat transfer for concentrations of nanoparticles of zirconium oxide below 0.07%; however, for increased concentrations (0.15%), the boiling heat transfer already began to deteriorate.

These techniques rely mostly on external modifications and do not influence the macrostructure of water itself. Otsuka et al. [23] investigated the effect of magnetic treatment on the physical properties of water but found no significant influence. The aim of the research presented in this paper was to examine glow-plasma water treatment (GPTW) as a potential method to improve the heat transfer coefficient during boiling. Water exposed to plasma is often colloquially referred to as nano-water. During this process, water molecules, which, due to their dipolar nature, tend to group together (form clusters called associates), are broken down into smaller, structured nanoclusters. The process itself was based on feeding demineralized water into the reactor vacuum chamber and exposing it to plasma at 38 °C. The plasma was obtained by a pulse generator, generating a magnetic field with a 280 GHz frequency, 50 mA current, and 600 V potential difference.

The possibilities of using GPTW are shown in Figure 1. The use of GPTW has already been reported in relation to disinfection [24] and the cryopreservation of biological samples [25]. This type of water is also used in cosmetology, due to the possibility of dissolving more chemical compounds, and even allows the dissolution of compounds that are practically insoluble in plain water, which makes

it possible to obtain highly-concentrated aqueous solutions of active substances. The food industry is the third branch in which GPTW is used [26,27], as it improves microbiological safety, stimulates plant growth, and increases the nutritional value [28–30]. However, to the best of authors' knowledge, no studies have been conducted to determine the possibility of using GPTW in industries using water as a cooling medium, for example in absorption or adsorption systems. In contrast to magnetic treated water, it was experimentally determined that low-pressure glow plasma may influence some of the physical properties of water such as pH, electric conductivity, and surface tension (Table 1). It was concluded [31] that the macrostructure of water is deteriorated due to exposure to plasma. However, an in-sight analysis of the papers related to the physical properties of water treated with plasma shows that there is no clear trend in its behavior. Most studies show that the pH for plasma-activated water increases. Similarly, the electrical conductivity increases, which may be associated with the formation of hydrogen and nitrate ions [32]. The density and viscosity of water are almost constant. The greatest discrepancy in the results was obtained for surface tension, where Mystkowska et al. [33] showed a significant increase (by over 30%), while studies [31] did not show a significant change.

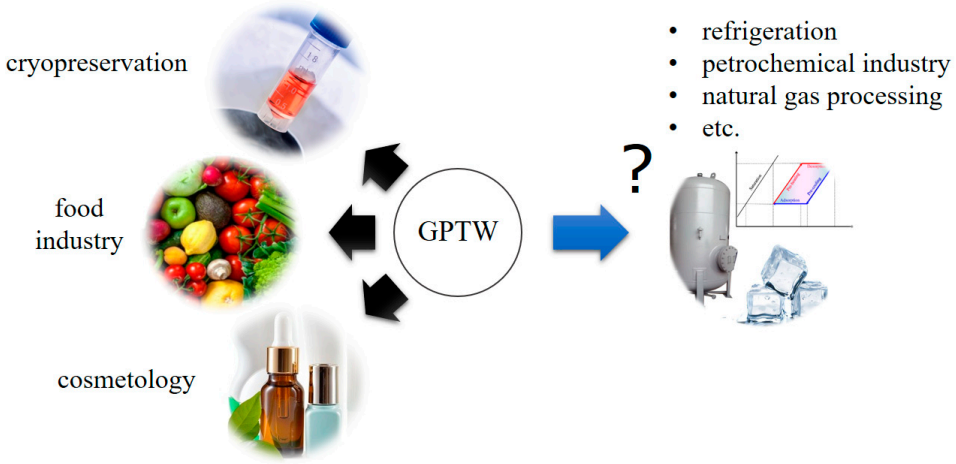

Figure 1. Possibilities of using glow plasma treated water (GPTW).

Table 1. Effect of low pressure glow plasma (LPGP) water treatment on selected physical properties.

Reference		pH	Density g/cm^3	Electric Conductivity µS/cm	Surface Tension mN/m	Viscosity Pa·s
[33]	DW	5.4	1.068	13.53	34	0.97
	GPTW	7.85	1.070	403	45	1.01
[24]	DW	8.43	-	-	-	-
	GPTW	4.15 7.14 [1]	-	-	-	-
[32]	RW	6.7 ± 0.00	-	160 ± 17.3	-	-
	GPTW	7.2 ± 0.1	-	246.7 ± 15.3	-	-
[31]	DW	5.56 ± 0.00	0.9980	-	72.20 ± 0.21	-
	GPTW 15 min	5.19 ± 0.03	0.9984	-	72.51 ± 0.27	-
	GPTW 30 min	5.19 ± 0.03	0.9984	-	72.47 ± 0.24	-
	GPTW 60 min	6.41 ± 0.01	0.9984	-	72.42 ± 0.23	-
	GPTW 90 min	5.83 ± 0.00	0.9984	-	72.42 ± 0.23	-

[1] after 24 h storage.

The purpose of this work is to conduct experimental research on the boiling process, aimed at determining the suitability of the application of GPTW in industries using the phase change process, such as refrigeration or petrochemicals, as presented in Figure 1. Therefore, the main experimental research did not focus on the physical parameters of water, although the boiling process depends on a number of these properties. In this context, the presented work is a new approach to the use of GPTW, and the tests performed are preliminary studies. In order to assess the potential of GPTW on enhancing the boiling heat transfer coefficient (HTC), experimental studies were carried out at atmospheric and reduced pressures of 7.5 kPa. The experiments were performed for a heat flux range from 10 to 70 kW/m^2. The boiling heat transfer coefficients for both GPTW and demineralized water were investigated, as well as the stability of the effect of the low-pressure glow plasma water treatment. In addition, the effect of plasma treatment on the thermal conductivity of water was investigated, as it is one of the key parameters controlling the heat exchange process, but at the same time, one that is not yet studied and not available in the literature. For the purposes of the study, two samples were produced, differing in plasma exposure time and pressure during the process. The first sample was made at a pressure of 5×10^{-3} mbar, by keeping it in the reactor chamber for 30 min, while the second was made at atmospheric pressure, but the duration of the process was extended to 60 min. After the process was completed, both GPTW were stored in sealed, Teflon containers at ambient temperature, without exposure to sunlight. In terms of the reactor operating settings, the samples obtained are identical to those used in [31,33], but differ in the length of the process.

2. Experimental Setup and Procedure

Studies of the boiling process were carried out on an experimental bench shown in Figure 2. It was composed of two brass flanges and a stainless steel tube with a diameter of 80 mm and a length of 300 mm. The boiling process of the substance occurred inside the tube, on a flat bottom flange made of brass, with a roughness of 0.05. Under the boiling surface, there was a flat heating element in the form of a resistance wire embedded in a heat-resistant mass. Current heating power was determined using an autotransformer, and measured with a wattmeter. Heat collection and the condensation of water took place in the upper part of the stand. The condenser was a copper multi-turn spiral with a diameter of 60 mm, through which cooling water flowed. The whole bench was insulated with polyurethane foam. A total of six temperature sensors for measuring the temperature of the heating surface (resistance thermometer PT100, 1/3 DIN), the temperature of the stainless steel tube (three thermocouples type K, class 1), and the temperature of the cooling water at the inlet and outlet from the condenser (two thermocouples type K, class 1) were installed in the stand. The vacuum value was measured with an absolute pressure gauge, together with a transducer, the Keller-Druck PAA33X-EV-120.

The methodology of the experiment consisted of supplying a stream of heat to the liquid with the amount resulting from the setting of the autotransformer and from the known area of the heating surface, and then reading all the measured temperatures and pressure in constant time steps. It was assumed that the pressure measured by the manometer was equal to that of the boiling liquid; on this basis, using the property tables, the saturation temperature for water was read. With the knowledge of overheating of the surface area and the heat flux (q) supplied to the fluid, the heat transfer coefficient (h) was determined using Equation (1). The experiment was conducted in such a way as to avoid complete evaporation of the liquid, which would result a sharp decrease in the heat transfer coefficient.

$$q = h \cdot (t_1 - t_2) \tag{1}$$

where t_1 is the temperature of the heating surface in °C, and t_2 is the boiling point temperature of the refrigerant, also in °C.

Temperature t_2 was not measured directly, but was determined based on the pressure inside the pressure vessel. It was assumed that the measured pressure would correspond to the saturation point at the equilibrium line between liquid and the saturated vapor (on the liquid surface). However, when

determining the heat transfer coefficient, reference should be made to the conditions prevailing on the heating surface, i.e., the contact of saturated liquid and heated surface. Therefore, the measured pressure was corrected for the hydrostatic pressure value of the liquid contained inside the test rig.

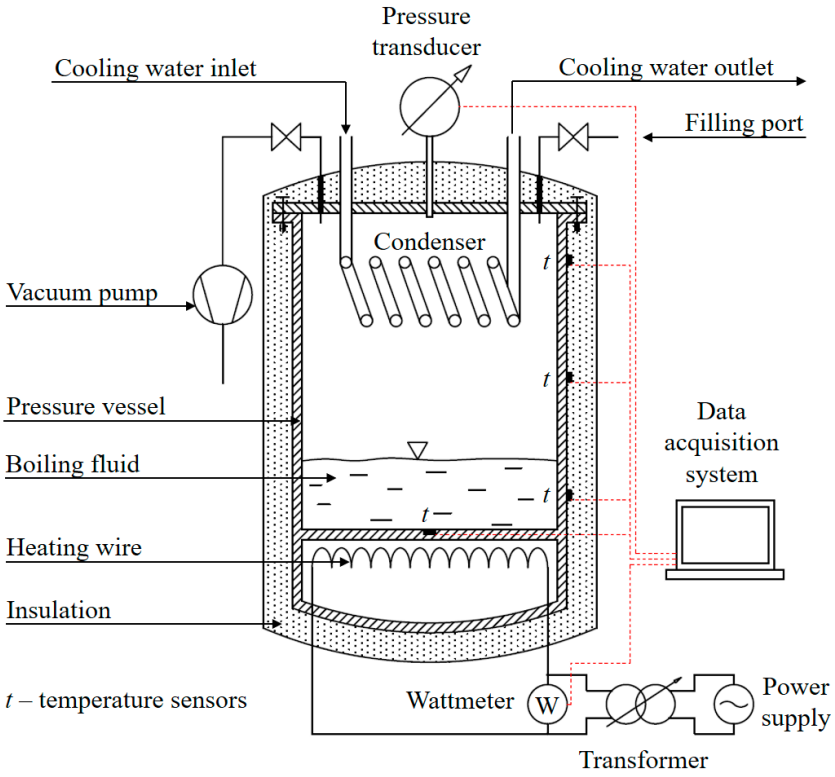

Figure 2. Experimental set-up.

Two samples of GPTW were used for the tests. The first was tested three days after preparation (the time necessary to received the sample from the manufacturer), and again after 14 days (results described as GPTW (1) and GPTW (2), respectively). The second sample was tested after one week (GPTW (3)). The purpose of the second sample was to examine whether air access in the plasma treatment process had an effect on its properties (especially HTC). Deionized water was also used for comparative purposes. Each time, the experimental setup was filled with 400 g of the fluid being tested. The amount of water during the testing of the boiling process at atmospheric pressure changed slightly, due to the need to release pressure from the inside of the tank in order to maintain constant pressure during the implementation of the subsequent measuring points. However, at reduced pressure, the amount of liquid did not change—the test rig was hermetically sealed. Three measurement series were made for each of the analyzed substances. Within one measurement series, the values of the HTC for each subsequent setting of the heat flux were made for about an hour from the moment the conditions inside the test stand were established. A measuring step of 10 min was used, which allowed us to obtain a cloud of about 20 measurements per measuring point, which was finally averaged using the least squares method.

3. Measurement Errors

While conducting the experiment, it was impossible to determine the actual value of the measured physical quantity. Each measurement was burdened with uncertainties resulting from imperfections in the measurement of the quantity caused by accidental changes in the results of the observations (accidental interactions), inaccurate determination of error corrections caused by systematic interactions, and incomplete knowledge of some physical phenomena (also systematic interactions). The standard uncertainty of type B was used to analyze the measurement uncertainties, which are burdened with

the results of the heat transfer coefficient. The HTC was determined using Equation (1). Assuming that the values appearing in the equation are independent of each other, it is possible to calculate the uncertainty of the complexity expressed in the following general formula:

$$u_c(Y) = \sqrt{\sum_{j=1}^{k}\left[\frac{\partial f}{\partial X_j}\left(\overline{X_1}, \overline{X_2}, \ldots, \overline{X_k}\right)\right]^2 u^2\left(\overline{X_j}\right)} \quad (2)$$

Standard uncertainty, assuming a rectangular distribution of errors, was calculated using the formula:

$$u(X) = \frac{\Delta X}{\sqrt{3}} \quad (3)$$

In addition, according to the International Norm of Uncertainty, introducing the notion of expanded uncertainty, given by the formula

$$U_c(Y) = k \cdot u_c(X) \quad (4)$$

the expansion coefficient $k = 2$ was assumed. Taking into account the above assumptions, the following formula was obtained to calculate the expanded uncertainty of the measurements affecting the value of the HTC:

$$U_c(h) = k \cdot \sqrt{\left(\frac{\partial h}{\partial P}\right)^2 \cdot u^2(P) + \left(\frac{\partial h}{\partial A}\right)^2 \cdot u^2(A) + \left(\frac{\partial h}{\partial t_1}\right)^2 \cdot u^2(t_1) + \left(\frac{\partial h}{\partial t_2}\right)^2 \cdot u^2(t_2)} \quad (5)$$

The values of measurement errors of the HTC, depending on the temperature difference and the heat flux density, are shown in Figure 3. The graph presents the absolute error values (on the left) and the relative error values, expressed as a percentage of the base value (on the right). The discontinuities in both graphs result from the use of a wattmeter with a variable measuring range. The change in the measuring range resulting from the increase in heat flux density caused jumps in the measurement errors for certain conditions. Maximum measurement errors (except for points in the natural convection area, i.e., for a temperature difference below 5 K) did not exceed 10%.

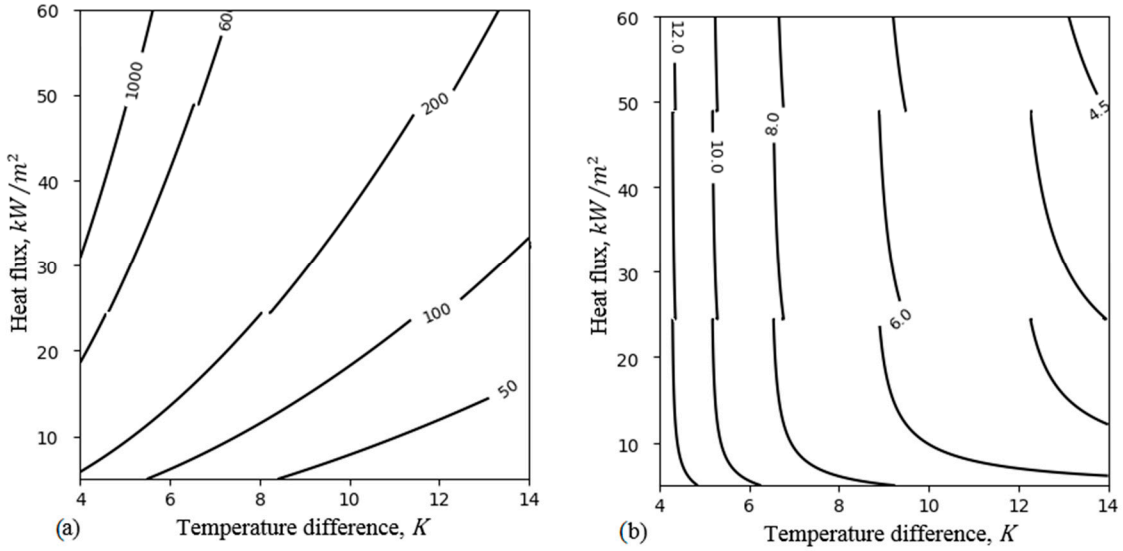

Figure 3. Maximum values of absolute (**a**) and relative (**b**) errors.

4. Results and Discussion

The research aimed to determine the HTC and to plot a fragment of the boiling curve of GPTW in two variants: at normal (atmospheric) pressure and at reduced pressure. In addition, all samples were subjected to thermal conductivity tests.

4.1. Boiling at Atmospheric Pressure

An examination of the boiling process of GPTW at normal pressure showed that the HTC for the analyzed fluids was very similar in the entire heat flux density range. The h values obtained by three samples of GPTW were almost the same as those for demineralized water (Figure 4). For a heat flux above 45 kW/m^2, there was no change in the HTC. Its slight changes were visible only for GPTW (3) in the range of heat fluxes below 45 kW/m^2. The maximum increase was equal to +250 W/m^{2}K (for q = 24–37 kW/m^2), which was 5–6% of the base value. Similarly, the boiling curve in the q–ΔT diagram was almost the same for all substances (Figure 5). The observed change in ΔT was from 0.1 to 0.4 K. The obtained results showed that nether low-pressure glow plasma water treatment nor air access during this process had a significant effect on changing the HTC. The change of HTC for all GPTW samples at normal pressure compared to demineralized water is very little, and within the uncertainty limits of the measurements.

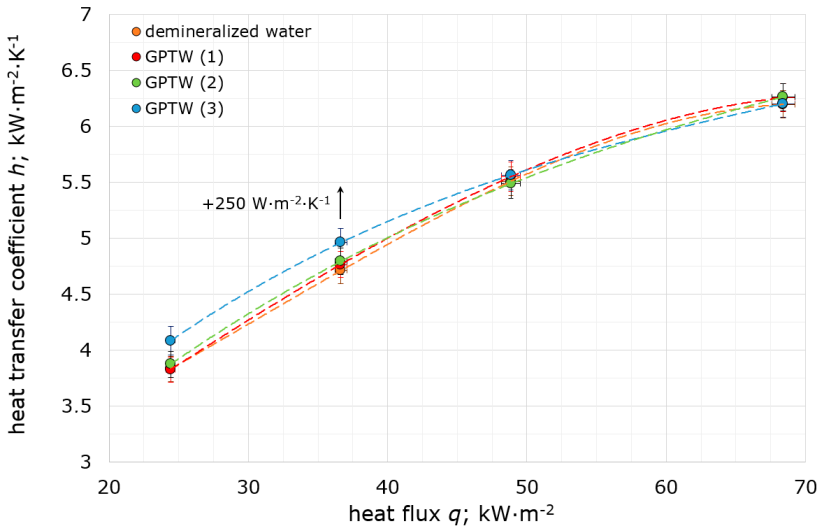

Figure 4. Nucleate boiling heat transfer coefficient (HTC) of GPTW at atmospheric pressure.

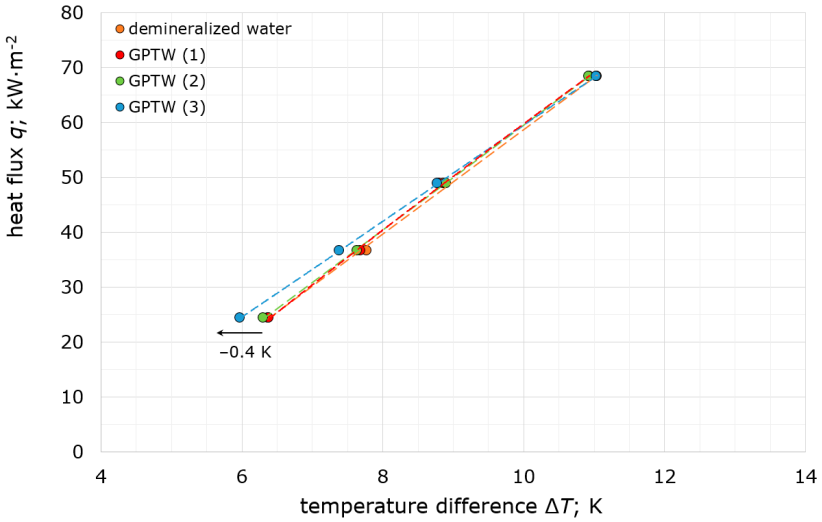

Figure 5. Boiling curves of GPTW at atmospheric pressure.

4.2. Boiling at Reduced Pressure

Figure 6 presents the results of measurements of the HTC for demineralized water and the tested samples of GPTW during boiling at reduced pressure (equal to 7.5 kPa). During the tests, the GPTW (1) obtained the lowest values of the HTC for the heat flux density range up to 60 kW/m^2, whereby the course of the boiling curve for demineralized water was maintained. The measuring points for the GPTW (2) also shifted downwards to the lower values of the HTC for a given heat flux density. In turn, the measuring points for demineralized water and the GPTW (3) almost overlapped. The values obtained for these two samples fell within the range of measurement errors. Large measurement errors in the range of low HTC and q values were caused by a relatively large measurement error of the temperature difference between the heating surface and the working medium. At the same time, the flattening of the measuring points for a heat flux of up to about 20 kW/m^2 suggested that no nucleate boiling took place, but only natural convection in the liquid volume.

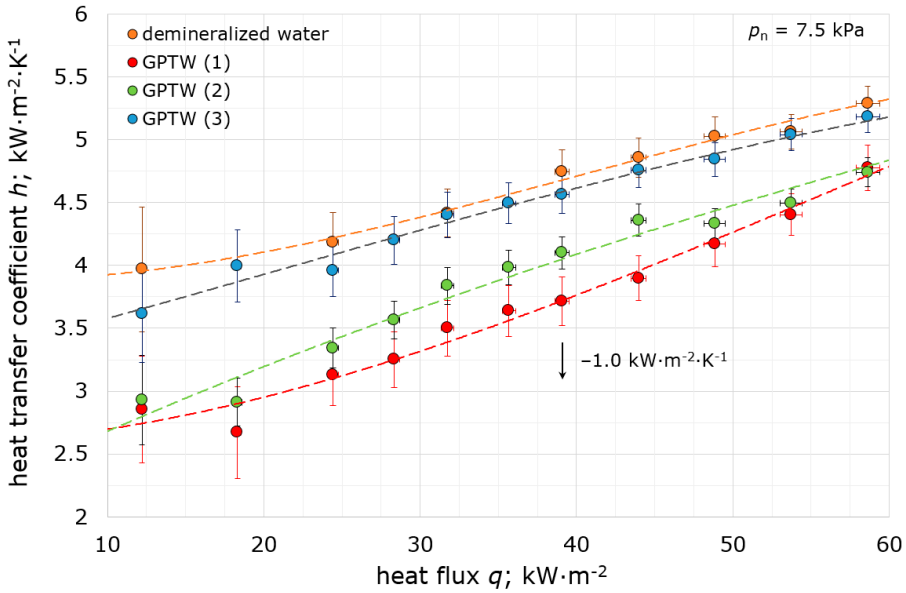

Figure 6. Nucleate boiling HTC of GPTW at reduced pressure.

A comparison of the experimental values of the HTC for GPTW (1) and GPTW (2) may indicate a gradual degradation of water subjected to the plasma treatment and a return of its parameters to deionized water. The results obtained for the GPTW (3) may suggest that the access of air in this process resulted in a lack of the effect of the process on the heat exchange during boiling, or a much faster degradation time of the nanocluster structure. The access of air in the plasma treatment process can lead to aeration of the liquid with a non-condensable gas, the presence of which may reduce the nucleation superheat required to initiate boiling. Therefore, it is possible to observe an increase in the HTC compared to GPTW (1) and (2) samples. The maximum decrease in the value of the heat transfer coefficient was 1.0 kW/(m^{2}K) (for q = 39 kW/m^2). As expected, the HTC increased for all samples as the heat flux density increased, and its maximum values for GPTW (1), (2), (3) and demineralized water were 4.8, 4.7, 4.2, and 5.3 kW/(m^{2}K), respectively. Another conclusion that can be assumed is that GPTW produced in near-vacuum conditions had a reduced ability to transfer heat compared with demineralized water. This is probably due to fewer nucleation sites. It may be deduced that the breakdown of the water structure from clusters into individual particles in the low-pressure glow plasma treatment process reduces the homogeneous nucleation sites associated with fluid density fluctuations.

The boiling curves of GPTW at reduced pressure are presented in Figure 7. The transition from the natural convection area to nucleate boiling occured later for samples of GPTW (1) and (2). Compared to

demineralized water, the transition point was shifted by around 2.3 K and 1.5 K to the right, respectively. This resulted in a decrease of the boiling HTC, as illustrated in the previous graph.

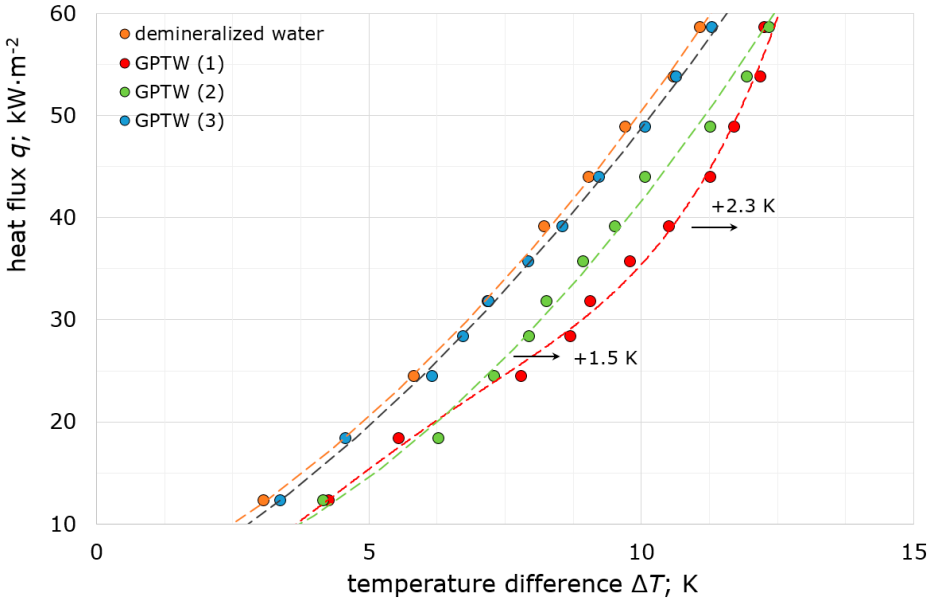

Figure 7. Boiling curves of GPTW at reduced pressure.

4.3. Thermal Conductivity

The HTC is mainly influenced by the thermal properties of the liquid, such as specific thermal conductivity k, kinematic viscosity υ, density ρ, or thermal expansion coefficient β. Studies [33] have shown that treating water with low-pressure glow plasma does not practically affect the density and viscosity of liquids. Due to the discrepancies between heat transfer coefficients for GPTW and deionized water, the effect of the process on thermal conductivity was investigated. Under the same heat exchange conditions, a larger amount of heat will flow through the substance, which is characterized by a higher thermal conductivity coefficient k. Similar to HTC, the tests were carried out at atmospheric and reduced pressure, and the liquid temperature was close to the ambient temperature (ranging from 23.8 °C to 25.2 °C). The obtained results were additionally compared with the data available for water in the REFProp v. 9.1 database [34].

Thermal conductivity tests were conducted using a KD2 Pro thermal properties analyzer. A standard single needle KS-1 sensor was used to measure thermal conductivity of all tested liquids. The sensor was immersed in the liquid in a vertical position, in the middle of the volume of the liquid being tested. A baseline reading time of one minute was used to reduce the amount of heat supplied to water during measurements, which is important for low viscosity liquids. The *Err* parameter was used to determine the quality of the measurement, which is a dimensionless measure of the goodness of matching the sensor calculation model to the measured values. It should be noted that the *Err* value is not a strict statistical indicator of the quality of the measurement, but more a qualitative quality indicator.

Most of the experimental results obtained (Figure 8) are below the reference line (REFProp data). The presented results show the lack of a clear trend regarding the thermal conductivity of GPTW in relation to deionized water, both at atmospheric and reduced pressure. The experimental values ranged from 0.558 to 0.631, which is consistent with the information provided for water in physical tables. The average values for GPTW and deionized water, respectively at atmospheric and reduced pressure, were 0.586, 0.593, 0.583, and 0.593 W/(mK).

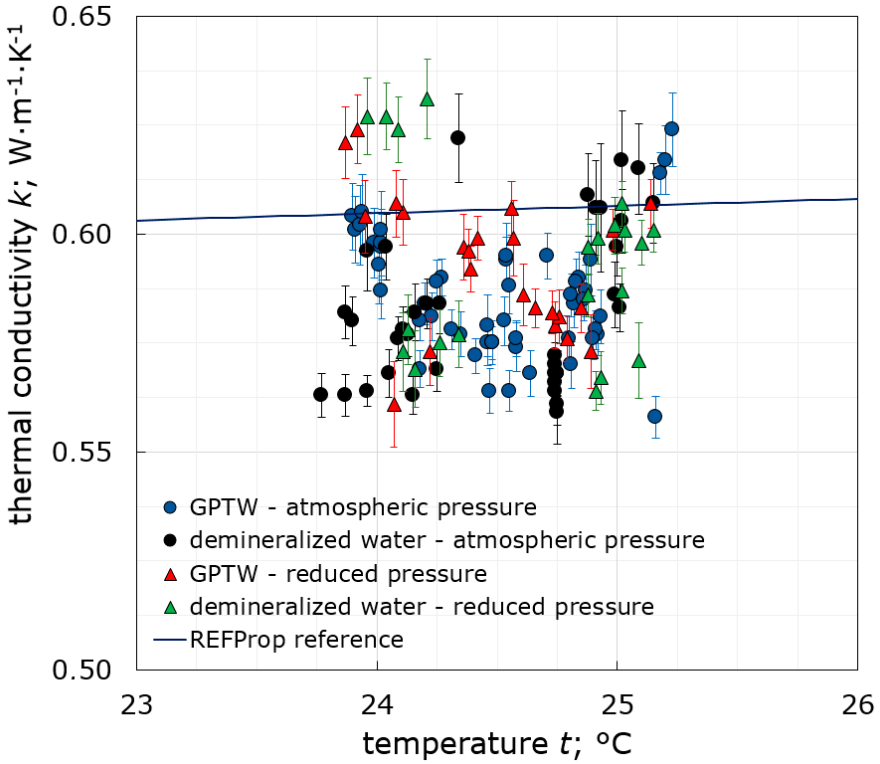

Figure 8. Thermal conductivity of GPTW and demineralized water.

Mystkowska et al. [33] also reported that the surface tension of GPTW is definitely higher than that of deionized water. This property has a key impact on the distribution of the forces that control the appearance, growth, and detachment of bubbles. Higher surface tension directly affects the shift of the transition point called onset of nucleate boiling (ONB) towards higher heat fluxes. Higher surface tension also means that the forces needed to depart bubbles from the nucleation surface are greater, thereby reducing bubble departure frequency. Both of these mechanisms may have caused the observed deterioration of heat exchange conditions, demonstrated in the study as a decrease in the value of HTC.

5. Conclusions

The paper presents experimental research on the pool boiling process of low-pressure glow plasma treated water. The tests were carried out at atmospheric and reduced pressure; their purpose was to determine the suitability of GPTW in technological processes by determining the value of the boiling heat transfer coefficient and its comparison with demineralized water. Tests at atmospheric pressure have shown that plasma treatment process does not significantly affect pool boiling of water, and the values of the heat transfer coefficient for both GPTW samples and demineralized water are almost identical. Significant deviations were observed during tests at reduced pressure. GPTW (1) shows a strong deterioration in the heat transfer coefficient, reaching up to 1.0 kW/m^2, which is a decrease of over 20% in relation to demineralized water. This is probably related to the change of the water structure from clusters to individual particles during low-pressure glow plasma treatment, which caused a reduction of homogeneous nucleation sites associated with fluid density fluctuations. The reason for the worsening heat exchange conditions may also be the increase in the surface tension of the liquid. Unfortunately, due to the insufficient amount of research devoted to the physical properties of GPTW, these are only assumptions which could not be confirmed experimentally. Definitely, more research in this field is needed to fully understand the behavior and processes occurring in plasma treated water. The boiling curve is shifted to higher temperature differences, which results in the extended range of natural convection and the subsequent transition to nucleate boiling. Studies show

that GPTW is not stable and fully returns to its initial state after about two weeks. Thus, its use in technological processes, especially phase change processes, is not justified. The above statement was also confirmed by tests of thermal conductivity. No significant change in thermal conductivity was observed for GPTW at either atmospheric and reduced pressure. Although the described studies show that the potential use of GPTW in phase change processes is not beneficial, it would be interesting to experimentally examine the effect of plasma on parameters controlling the process of bubble formation and growth, such as contact angle, surface tension, or thermal diffusivity, which may constitute future scientific research on GPTW.

Author Contributions: Data curation, Z.R. and P.D.; Formal analysis, B.G.; Methodology, B.G.; Visualization, B.G.; Writing—original draft, B.G., Z.R. and P.D. All authors have read and agreed to the published version of the manuscript.

Funding: Financial support from Wrocław University of Science and Technology, grants number 0402/175/18 and 049U/0070/19 is greatly appreciated. Authors would also like to thank Zdzisław Oszczęda and Nanolaboratory Nantes for preparing and providing the samples of GPTW.

Conflicts of Interest: The authors declare no conflicts of interest.

Nomenclature

A	area (m^2)
h	heat transfer coefficient ($kW \cdot m^{-2} \cdot K^{-1}$)
P	heating power (W)
q	heat flux ($kW \cdot m^{-2}$)
t	temperature (°C or K)
Abbreviations	
DW	Demineralized Water
GPTW	Low-pressure glow plasma treated water
HTC	Heat transfer coefficient
LPGP	Low-pressure glow plasma
RW	Raw water

References

1. Park, I.S.; Park, S.M.; Ha, J.S. Design and application of thermal vapor compressor for multi-effect desalination plant. *Desalination* **2005**, *182*, 199–208. [CrossRef]
2. Zajaczkowski, B. Optimizing performance of a three-bed adsorption chiller using new cycle time allocation and mass recovery. *Appli. Ther. Eng.* **2016**. [CrossRef]
3. Pan, Q.; Peng, J.; Wang, H.; Sun, H.; Wang, R. Experimental investigation of an adsorption air-conditioner using silica gel-water working pair. *Sol. Energy* **2019**, 64–71. [CrossRef]
4. Ren, J.; Qian, Z.; Yao, Z.; Gan, N.; Zhang, Y. Thermodynamic Evaluation of LiCl-H_2O and LiBr-H_2O Absorption Refrigeration Systems Based on a Novel Model and Algorithm. *Energies* **2019**, *12*, 3037. [CrossRef]
5. López-Zavala, R.; Velázquez-Limón, N.; González-Uribe, L.A.; Aguilar-Jiménez, J.A.; Alvarez-Mancilla, J.; Acuña, A.; Islas, S. A novel LiBr/H_2O absorption cooling and desalination system with three pressure levels. *Int. J. Refrig.* **2019**, *99*, 469–478. [CrossRef]
6. Dong, J.; Wang, W.; Han, Z.; Ma, H.; Deng, Y.; Su, F.; Xinxiang, P. Experimental investigation of the steam ejector in a single-effect thermal vapor compression desalination system driven by a low-temperature heat source. *Energies* **2018**, *11*, 2282. [CrossRef]
7. Giraud, F. Vaporization of Water at Subatmospheric Pressure: Fundamentals of Boiling Phenomena and Path towards the Design of Compact Evaporators for Sorption Chillers. Ph.D. Thesis, École Doctorale MEGA, Lyon, France, 2015.
8. Mori, S.; Aznam, S.M.T.; Okuyama, K. Enhancement of the critical heat flux in saturated pool boiling of water by nanoparticle-coating and a honeycomb porous plate. *Int. J. Heat Mass Transf.* **2015**, *80*, 1–6. [CrossRef]
9. Xu, P.; Li, Q.; Xuan, Y. Enhanced boiling heat transfer on composite porous surface. *Int. J. Heat Mass Transf.* **2015**, *80*, 107–114. [CrossRef]

10. Jun, S.; Kim, J.; Son, D.; Kim, H.Y.; You, S.M. Enhancement of Pool Boiling Heat Transfer in Water Using Sintered Copper Microporous Coatings. *Nucl. Eng. Technol.* **2016**, *48*, 932–940. [CrossRef]
11. Halon, T.; Zajaczkowski, B.; Michaie, S.; Rulliere, R.; Bonjour, J. Enhanced tunneled surfaces for water pool boiling heat transfer under low pressure. *Int. J. Heat Mass Transf.* **2018**. [CrossRef]
12. Kiyomura, I.S.; Manetti, L.L.; da Cunha, A.P.; Ribatski, G.; Cardoso, E.M. An analysis of the effects of nanoparticles deposition on characteristics of the heating surface and ON pool boiling of water. *Int. J. Heat Mass Transf.* **2017**. [CrossRef]
13. Wen, D. Influence of nanoparticles on boiling heat transfer. *Appl. Therm. Eng.* 2012. [CrossRef]
14. Jones, B.J.; McHale, J.P.; Garimella, S.V. The Influence of Surface Roughness on Nucleate Pool Boiling Heat Transfer. *Int. J. Heat Transf.* **2009**, *131*, 121009. [CrossRef]
15. Yang, Y.; Ji, X.; Xu, J. Pool boiling heat transfer on copper foam covers with water as working fluid. *Int. J. Therm. Sci.* **2010**, *49*, 1227–1237. [CrossRef]
16. Shi, B.; Wang, Y.B.; Chen, K. Pool boiling heat transfer enhancement with copper nanowire arrays. *Appl. Therm. Eng.* **2015**, *75*, 115–121. [CrossRef]
17. Wang, H.; Yang, Y.; He, M.; Qiu, H. Subcooled flow boiling heat transfer in a microchannel with chemically patterned surfaces. *Int. J. Heat Mass Transf.* **2019**. [CrossRef]
18. McGillis, W.R.; Fitch, J.S.; Hamburgen, W.R.; Carey, V.P. *Pool Boiling Enhancement Techniques for Water at Low Pressure*; WRL Research Report 90/9; IEEE: Piscataway, NJ, USA, 1990; p. 33.
19. You, S.M.; Kim, J.H.; Kim, K.H. Effect of nanoparticles on critical heat flux of water in pool boiling heat transfer. *Appl. Phys. Lett.* **2003**, *83*, 3374–3376. [CrossRef]
20. Kwark, S.M.; Kumar, R.; Moreno, G.; Yoo, J.; You, S.M. Pool boiling characteristics of low concentration nanofluids. *Int. J. Heat Mass Transf.* **2010**, *53*, 972–981. [CrossRef]
21. Kim, H.; Ahn, H.S.; Kim, M.H. On the Mechanism of Pool Boiling Critical Heat Flux Enhancement in Nanofluids. *J. Heat Transf.* **2010**, *132*, 061501. [CrossRef]
22. Chopkar, M.; Das, A.K.; Manna, I.; Das, P.K. Pool boiling heat transfer characteristics of ZrO_2-water nanofluids from a flat surface in a pool. *Heat Mass Transf.* **2008**, *44*, 999–1004. [CrossRef]
23. Otsuka, I.; Ozeki, S. Does Magnetic Treatment of Water Change Its Properties? *J. Phys. Chem. B* **2006**, *110*, 1509–1512. [CrossRef] [PubMed]
24. Rashmei, Z.; Bornasi, H.; Ghoranneviss, M. Evaluation of treatment and disinfection of water using cold atmospheric plasma. *J. Water Health* **2016**, *14*, 609–616. [CrossRef] [PubMed]
25. Murawski, M.; Schwarz, T.; Grygier, J.; Patkowski, K.; Oszczęda, Z.; Jelkin, I.; Kosiek, A.; Gruszecki, T.M.; Szymanowska, A.; Skrzypek, T.; et al. The utility of nanowater for ram semen cryopreservation. *Exp. Biol. Med.* **2015**, *240*, 611–617. [CrossRef] [PubMed]
26. Coutinho, N.M.; Silveira, M.R.; Rocha, R.S.; Moraes, J.; Ferreira, M.V.S.; Pimentel, T.C.; Freitas, M.Q.; Silva, M.C.; Raices, R.S.L.; Ranadheera, C.; et al. Cold plasma processing of milk and dairy products. *Trends Food Sci. Technol.* **2018**, *74*, 56–68. [CrossRef]
27. Mandal, R.; Singh, A.; Singh, A.P. Recent developments in cold plasma decontamination technology in the food industry. *Trends Food Sci. Technol.* **2018**, *80*, 93–103. [CrossRef]
28. Hawrylak-Nowak, B.; Dresler, S.; Matraszek-Gawron, R.; Oszczęda, Z.; Pogorzelec, M. The water treated with low-frequency low-pressure glow plasma enhances the phytoavailability of selenium and promotes the growth of selenium-treated cucumber plants. *Acta Sci. Pol. Hortorum Cultus* **2018**, *17*, 109–116. [CrossRef]
29. Pisulewska, E.; Ciesielski, W.; Jackowska, M.; Gąstoł, M.; Oszczęda, Z.; Tomasik, P. Cultivation of peppermint (*Mentha piperita rubescens*) using water treated with low-pressure, low-temperature glow plasma of low frequency. *Electron. J. Polish Agric. Univ.* **2018**, *21*. [CrossRef]
30. Patange, A.; Lu, P.; Boehm, D.; Cullen, P.J.; Bourke, P. Efficacy of cold plasma functionalised water for improving microbiological safety of fresh produce and wash water recycling. *Food Microbiol.* **2019**, *84*, 103226. [CrossRef]
31. Bialopiotrowicz, T.; Ciesielski, W.; Domanski, J.; Doskocz, M.; Khachatryan, K.; Fiedorowicz, M.; Graz, K.; Koloczek, H.; Kozak, A.; Oszczeda, Z. Structure and Physicochemical Properties of Water Treated with Low-Temperature Low-Frequency Glow Plasma. *Curr. Phys. Chem.* **2016**, *6*, 312–320. [CrossRef]
32. Van Nguyen, D.; Ho, P.Q.; Van Pham, T.; Van Nguyen, T.; Kim, L. A study on treatment of surface water using cold plasma for domestic water supply. *Environ. Eng. Res.* **2019**, *24*, 412–417. [CrossRef]

33. Mystkowska, J.; Dabrowski, J.R.; Kowal, K.; Niemirowicz, K.; Car, H. Physical and chemical properties of deionized water and saline treated with low-pressure and low-temperature plasma. *Chemik* **2013**, *67*, 719–724.
34. Lemmon, E.W.; Bell, I.H.; Huber, M.L.; McLinden, M.O. *NIST Standard Reference Database: REFPROP Reference Fluid Thermodynamic and Transport Properties*, version 9.1 2018; National Institute of Standards and Technology: Gaithersburg, MD, USA, 2018.